

Truncations of a class of pseudo-Hermitian operators

Maxim Derevyagin*, Luca Perotti†, Michał Wojtylak§

* *University of Mississippi, Department of Mathematics, Hume Hall 305,
P. O. Box 1848, University, MS 38677-1848, USA. derevyagin.m@gmail.com*

† *Department of Physics, Texas Southern University,
Houston, Texas 77004 USA. perottil@tsu.edu and*

§ *Jagiellonian University, Faculty of Mathematics and Computer Science,
Lojasiewicza 6, 30-348 Kraków. michal.wojtylak@gmail.com*

(Dated: July 16, 2018)

We consider the class of non-Hermitian operators represented by infinite tridiagonal matrices, selfadjoint in an indefinite inner product space with one negative square. We approximate them with their finite truncations. Both infinite and truncated matrices have eigenvalues of nonpositive type: either a single one on the real axis or a couple of complex conjugate ones. As a tool to evaluate the reliability of the use of truncations in numerical simulations, we give bounds for the rate of convergence of their eigenvalues of nonpositive type. Numerical examples illustrate our results.

MSC 2010 numbers: 47B36, 47B50

PACS numbers: 02.30.Tb, 11.30.Er, 03.65.-w

I. INTRODUCTION

The Hamiltonian H of a physical system represents its energy, which is a real observable. It is therefore required that the expectation values of the quantum operator H be real [1]. This can be guaranteed by imposing that H be Hermitian, $H = H^\dagger$, as it is known that the spectrum of a Hermitian operator is real and its eigenvectors form a complete orthogonal set [2].

It is on the other hand known that Hermiticity is not a necessary condition for a real spectrum [3]: a large number of one-dimensional non-Hermitian potentials, both real and complex, invariant under the simultaneous actions of the parity P (space reflection) and time reflection T operators [4] have been found to admit energies that are real and discrete.

The matter is not a idle one, as non-Hermitian PT-invariant operators find applications in many areas of theoretical physics: “optical” or “average” potentials in nuclear physics [5], quantum field theories [6], scattering problems [7], localization-delocalization transitions in superconductors [8], defraction of atoms by standing light waves [9], as well as the study of solitons on a complex Toda lattice [10].

Unfortunately, PT-invariance is neither necessary nor sufficient to ensure the reality of the spectrum; however, it has been conjectured [3] that PT invariant Hamiltonians possess real discrete eigenvalues if the PT symmetry is unbroken i.e. if the energy eigenstates are also eigenstates of the operator PT. When the PT-symmetry is broken and the Hamiltonian is real there instead are energy eigenvalues that are complex conjugate pairs. However, no general condition has been found for the breakdown of the PT-symmetry.

In this contest, it has been pointed out that a necessary, but not sufficient, condition for the spectrum to be real and discrete is the η -pseudo-Hermiticity, $\eta H \eta^{-1} = H^\dagger$, of the Hamiltonian, where η is a Hermitian linear automorphism [11]. The property is also known as selfadjointness in an indefinite inner product space, see [12–14]. The eigenvectors of H are in this case η -orthogonal, i.e. they are orthogonal according to the η -distorted inner-product $\langle \psi | \eta \psi \rangle$.

Several PT-symmetric potentials have been found to be P-pseudo-Hermitian [15] and classes of non-Hermitian Hamiltonians -both PT-symmetric and non-PT-symmetric- appear to be pseudo-Hermitian under $\eta = e^{-\theta p}$ where $\theta \in \mathbb{R}$ and $p = i \frac{d}{dx}$, ($\hbar = 1$) is the momentum operator (the transformation generated by η is an imaginary shift: $\eta x \eta^{-1} = x + i\theta$, $\eta p \eta^{-1} = p$) [16], or $\eta = e^{-\varphi(x)}$ where $\varphi(x)$ is a C^1 function of x (the transformation is a complex gauge-like one) [17].

It is thus still a case by case procedure to check whether the eigenvalues of an operator are all real. This does not usually cause big practical problems when dealing with a single operator. The situation changes when we have to consider classes of operators. Procedures have been developed for families of operators acting on spaces with finite bases, see e.g. Ref. [18] whose author considers a one parameter family of PT-symmetric matrices $M(\varepsilon)$, with a perturbation parameter $\varepsilon \in \mathbb{R}$ which destroys Hermiticity while it respects PT-invariance.

Here we consider the case when for numerical simulations an operator H acting on a space with an infinite basis needs to be truncated and study the rate of convergence to their asymptotic value of those eigenvalues that for

truncated matrices may happen to be non-real. The operator $H = H_{[0,\infty)}$ is given by a non-symmetric Jacobi matrix

$$H_{[0,\infty)} = \begin{pmatrix} a_0 & -b_0 & & & \\ b_0 & a_1 & b_1 & & \\ & b_1 & a_2 & b_2 & \\ & & b_2 & a_3 & \ddots \\ & & & \ddots & \ddots \end{pmatrix}, \quad (\text{I.1})$$

with bounded, real sequences $(a_j)_{j=0}^\infty$, $(b_j)_{j=0}^\infty$, the sequence $(b_j)_{j=0}^\infty$ being additionally strictly positive. Its finite truncations are of the form

$$H_{[0,n]} = \begin{pmatrix} a_0 & -b_0 & & & \\ b_0 & a_1 & b_1 & & \\ & b_1 & a_2 & \ddots & \\ & & \ddots & \ddots & b_{n-1} \\ & & & b_{n-1} & a_n \end{pmatrix}, \quad (\text{I.2})$$

and

$$\eta = \text{diag}(-1, 1, 1, \dots).$$

Due to the fundamental theorem of Pontryagin [19] each the operators $H_{[0,n]}$ has, generically, either a unique single eigenvalue λ_n on the real axis with the eigenvector f_n satisfying $\langle f_n | \eta f_n \rangle \leq 0$ or a single couple of complex conjugate eigenvalues $\lambda_n \in \mathbb{C}^+$, $\bar{\lambda}_n \in \mathbb{C}^-$ (to avoid confusion with the conventions used in some of the papers we quote, we note that here and in the following $\langle x|y \rangle$ always denotes the usual inner product –either in \mathbb{C}^n or in ℓ^2 – *linear with respect to the second variable*). The remaining part of the spectrum of $H_{[0,n]}$ is real. The same is true for the spectrum of the infinite matrix $H_{[0,\infty)}$ with the eigenvalue λ_∞ , see Section II for details. The character of the convergence $\lambda_n \rightarrow \lambda_\infty$ is the main topic of our paper.

Our approach makes use of analytic representations of the function

$$m_{[0,\infty)}(z) = -\langle e_0 | (H_{[0,\infty)} - z)^{-1} e_0 \rangle, \quad (\text{I.3})$$

which contains the full information about the spectrum of $H_{[0,\infty)}$ and of its $[n - 1/n]$ Padé approximants

$$m_{[0,n]}(z) = -\langle e_0 | (H_{[0,n]} - z)^{-1} e_0 \rangle. \quad (\text{I.4})$$

In particular, λ_n (λ_∞) is a pole of $m_{[0,n]}(z)$ ($m_{[0,\infty)}$, respectively) and it can be characterized in analytic terms. Due to the locally uniform convergence of $m_{[0,n]}$ to $m_{[0,\infty)}$ [20], the sequence $(\lambda_n)_{n=0}^\infty$ converges to λ_∞ (Corollary II.5). Our main interest is the rate of this convergence. In particular we show its dependence of the placement of the eigenvalue λ_∞ in $\mathbb{C}^+ \cup \mathbb{R}$.

Our paper is organized as follows:

- We give various analytic representations of the function (I.3), choosing in particular as our starting point

$$\frac{-1}{m_{[0,\infty)}(z)} = a_0 - z + b_0^2 \int_{t_3}^{t_4} \frac{d\mu(t)}{t - z},$$

where μ is some probability measure, see Theorem II.1.

- In the case $\lambda_\infty \notin [t_3, t_4]$ we show that the convergence rate of λ_n to λ_∞ is exponential, with the base of the exponent increasing with the distance of λ_∞ from $[t_3, t_4]$: see Theorem III.3 below.
- However, the λ_n 's tend to arrange themselves in branches spiraling into λ_∞ and some of these branches can get trapped in the real axis for a number of iterations n_0 which can be relatively large when λ_∞ is close to $[t_3, t_4]$. We show examples with different numbers of branches and compute an estimate for n_0 in Theorem A.1.
- In the case when $\lambda_\infty \in [t_3, t_4]$ we build an example to show that the convergence rate is in general worse than exponential.
- In the concluding remarks we review the possible cases from the numerical point of view.

II. HOLOMORPHIC REPRESENTATIONS OF THE m -FUNCTION

We start with reviewing the spectral properties of the matrices $H_{[0,n]}$ and $H_{[0,\infty]}$. The matrix $H_{[0,n]}$ is selfadjoint in the indefinite inner-product space with the fundamental symmetry given by $\eta_n = [-1] \oplus I_n$ (η_n -pseudo-Hermitian). Consequently one of the following four possibilities applies:

- (i) $H_{[0,n]}$ is similar to a diagonal matrix with real entries, except two complex conjugate entries $\lambda_n \in \mathbb{C}^+$, $\bar{\lambda}_n \in \mathbb{C}^-$. The eigenvectors f_n, g_n corresponding to the eigenvalues $\lambda_n, \bar{\lambda}_n$ of $H_{[0,n]}$ satisfy $\langle f_n | \eta_n f_n \rangle = \langle g_n | \eta_n g_n \rangle = 0$, $\langle f_n | \eta_n g_n \rangle \neq 0$.
- (ii) $H_{[0,n]}$ is similar to a diagonal matrix with real entries and there is precisely one eigenvalue λ_n with the corresponding eigenvector f_n satisfying $\langle f_n | \eta_n f_n \rangle < 0$.
- (iii) $H_{[0,n]}$ is similar to a block-diagonal matrix with all the blocks real and one-dimensional, except one block of the form

$$\begin{pmatrix} \lambda_n & 1 \\ 0 & \lambda_n \end{pmatrix} \text{ with } \lambda_n \in \mathbb{R}.$$

The eigenvector f_n corresponding to the eigenvalue λ_n of $H_{[0,n]}$ satisfies $\langle f_n | \eta_n f_n \rangle = 0$.

- (iv) $H_{[0,n]}$ is similar to a block-diagonal matrix with all the blocks real and one-dimensional, except one block of the form

$$\begin{pmatrix} \lambda_n & 1 & 0 \\ 0 & \lambda_n & 1 \\ 0 & 0 & \lambda_n \end{pmatrix} \text{ with } \lambda_n \in \mathbb{R}.$$

The eigenvector f_n corresponding to the eigenvalue λ_n of $H_{[0,n]}$ satisfies $\langle f_n | \eta_n f_n \rangle = 0$.

The cases (iii) and (iv) are non-generic, i.e. the set of all matrices $H_{[0,n]}$ for which one of them applies has measure zero. We refer the reader to [14] for the full canonical form of matrices selfadjoint in indefinite inner-product spaces, which gives also a full description of the eigenvectors. We observe that the matrix $H_{[0,n]}$ may jump back and forth with n among the four types above.

The spectral properties of the infinite matrix $H_{[0,\infty]}$, understood as an operator on ℓ^2 , are more tricky: we refer the reader to [21, 22] for a full description and for canonical models. Here we note only that again there are essentially two possibilities:

- (i') $H_{[0,\infty]}$ is similar to an orthogonal sum of a bounded selfadjoint operator in a Hilbert space and a diagonal matrix with two complex conjugate entries $\lambda_n \in \mathbb{C}^+$, $\bar{\lambda}_n \in \mathbb{C}^-$. The eigenvectors f_n, g_n corresponding to the eigenvalues $\lambda_n, \bar{\lambda}_n$ of $H_{[0,\infty]}$ satisfy $\langle f_n | \eta_n f_n \rangle = \langle g_n | \eta_n g_n \rangle = 0$, $\langle f_n | \eta_n g_n \rangle \neq 0$.
- (ii') The spectrum of $H_{[0,\infty]}$ is real and $H_{[0,\infty]}$ has a (unique) real eigenvalue with the corresponding eigenvector f_∞ satisfying $\langle f_\infty | \eta f_\infty \rangle \leq 0$.

In the (ii') case the Jordan chain corresponding to λ_∞ is again of length not greater than three.

Now we specify the theory developed in [20, 23, 24] to the case we are dealing with in the present work. Besides the matrices $H_{[0,\infty]}$ and $H_{[0,n]}$ defined in (I.1) and (I.2), we shall use the following truncations of the matrix $H_{[0,\infty]}$

$$H_{[1,n]} = \begin{pmatrix} a_1 & b_1 & & & \\ b_1 & a_1 & & & \\ & & \ddots & & \\ & & \ddots & \ddots & b_{n-1} \\ & & & b_{n-1} & a_n \end{pmatrix}, \quad n = 1, 2, \dots \quad (\text{II.1})$$

Furthermore, $H_{[1,\infty]}$ will stand for the infinite, symmetric Jacobi matrix with $(a_j)_{j=1}^\infty$ on the main and $(b_j)_{j=1}^\infty$ on the second diagonals. Similarly to (I.3) and (I.4) we define the functions

$$m_{[1,n]}(z) = \langle e_1 | (H_{[1,n]} - z)^{-1} e_1 \rangle, \quad m_{[1,\infty]}(z) = \langle e_1 | (H_{[1,\infty]} - z)^{-1} e_1 \rangle. \quad (\text{II.2})$$

Here e_j stands for the j -th vector of the canonical basis of ℓ^2 . We call the functions appearing in (I.3), (I.4) and (II.2) the m -functions of the corresponding Jacobi matrix. We refer the reader to [25] for a treatment of m -functions

of symmetric Jacobi matrices appearing in (II.2). The functions $m_{[1,n]}$ ($n \in \mathbb{Z}_+$) and $m_{[1,\infty]}$ are analytic in the open upper half-plane \mathbb{C}^+ . The function $m_{[0,\infty]}$ ($m_{[0,n]}$) is analytic in the upper half-plane, except λ_∞ (λ_n , respectively).

Moreover, the Schur complement argument provides the following crucial relations [24, 25]

$$m_{[0,n]}(z) = \frac{1}{z - a_0 - b_0^2 m_{[1,n]}(z)}, \quad z \in \mathbb{C}^+ \setminus \{\lambda_n\}, \quad n \in \mathbb{Z}_+, \quad (\text{II.3})$$

$$m_{[0,\infty]}(z) = \frac{1}{z - a_0 - b_0^2 m_{[1,\infty]}(z)}, \quad z \in \mathbb{C}^+ \setminus \{\lambda_\infty\}. \quad (\text{II.4})$$

Let us now recall the definition of the class \mathcal{N}_1 . By \mathcal{N}_1 we define the set of generalized Nevanlinna functions with one negative square, that is the functions of one of the three forms

$$\frac{(z - \alpha)(z - \bar{\alpha})}{(z - \beta)(z - \bar{\beta})} \varphi(z), \quad (\text{II.5})$$

$$\frac{1}{(z - \beta)(z - \bar{\beta})} \varphi(z), \quad (\text{II.6})$$

$$(z - \alpha)(z - \bar{\alpha}) \varphi(z), \quad (\text{II.7})$$

where α, β are complex numbers and φ is a Nevanlinna function, i.e. φ is holomorphic in \mathbb{C}_+ and maps \mathbb{C}_+ into $\mathbb{C}^+ \cup \mathbb{R}$. We refer the reader to [26, 27] for equivalent definitions. Let us now formulate the theorem which fixes the subclass of \mathcal{N}_1 functions to be investigated in the present work:

Theorem II.1 *Let m be a meromorphic function in the open upper half plane. The following conditions are equivalent.*

(i) *There exist $\lambda_\infty \in \mathbb{C}^+ \cup \mathbb{R}$, $d \in \mathbb{R}$ and a nontrivial Borel measure σ having all moments finite and supported on an interval $[t_1, t_2]$ such that*

$$m(z) = \frac{1}{(z - \lambda_\infty)(z - \bar{\lambda}_\infty)} \left(z + d + \int_{t_1}^{t_2} \frac{d\sigma(t)}{t - z} \right), \quad (\text{II.8})$$

(ii) *There exist $a_0 \in \mathbb{R}$, $b_0 > 0$ and a nontrivial Borel probability measure μ having all moments finite and supported on an interval $[t_3, t_4]$ such that*

$$\frac{-1}{m(z)} = a_0 - z + b_0^2 \int_{t_3}^{t_4} \frac{d\mu(t)}{t - z} \quad (\text{II.9})$$

(iii) *There exist a matrix $H_{[0,\infty]}$ of the form (I.1) with bounded entries $a_j \in \mathbb{R}$, $b_j > 0$, $j \in \mathbb{Z}_+$ such that*

$$m(z) = m_{[0,\infty]}(z) := - \langle e_0 | (H_{[0,\infty]} - z)^{-1} e_0 \rangle. \quad (\text{II.10})$$

Furthermore, the parameters λ_∞ and d and the measure σ in (i), a_0, b_0 and μ in (ii), and a_j, b_j , $j \in \mathbb{Z}_+$ in (iii) are uniquely determined; the numbers a_0 and b_0 in statements (ii) and (iii) coincide and λ_∞ from statement (i) is the (unique) eigenvalue of nonpositive type of the operator $H_{[0,\infty]}$ from statement (iii).

Proof. The equivalence (ii) \Leftrightarrow (iii) is a consequence of equation (II.4) and the classical theory which sets a correspondence between the functions $m_{[1,\infty]}$ and the Jacobi matrices $H_{[1,\infty]}$, see e.g. [25, 28].

(iii) \Rightarrow (i) Let $m = m_{[0,\infty]}$. From the construction in [21] it follows that m belongs to the class \mathcal{N}_1 and hence it has one of the forms (II.5)–(II.7).

Furthermore, expanding the resolvent into a geometric series at infinity one sees that m necessarily possesses an asymptotic expansion at infinity

$$m(z) = - \langle e_0 | (H_{[0,\infty]} - z)^{-1} e_0 \rangle = \frac{1}{z} - \frac{s_1}{z^2} - \dots - \frac{s_{2n}}{z^{2n+1}} - \dots, \quad (\text{II.11})$$

with $s_j \in \mathbb{R}$ ($j = 1, 2, \dots$) (see [20, 24]). Comparing the forms (II.5)–(II.7) with (II.11), one gets by the Hamburger–Nevanlinna theorem [28] that the function φ in (II.5)–(II.7) can be represented in the form

$$\varphi(z) = z + d + \int_{t_1}^{t_2} \frac{d\sigma(t)}{t - z}, \quad (\text{II.12})$$

where $d \in \mathbb{R}$, and σ is a measure with all moments finite. Furthermore, comparing the expansions of (II.5), (II.6) and (II.7) with (II.11) we can see that case (II.6) applies. In consequence,

$$m(z) = \frac{1}{(z - \lambda_\infty)(z - \bar{\lambda}_\infty)} \left(z + d + \int_{t_1}^{t_2} \frac{d\sigma(t)}{t - z} \right), \quad (\text{II.13})$$

Observe that the measure σ cannot be a finitely supported (trivial) measure, since $b_j > 0$ for all $j \in \mathbb{Z}_+$ and in consequence neither $m_{[1, \infty)}$ nor $m_{[0, \infty)}$ are rational functions. The uniqueness of the parameters λ_∞ and d and of the measure σ follows from the theory of \mathcal{N}_1 functions, see e.g. [26]. The fact that λ_∞ is the unique eigenvalue of nonpositive type of $H_{[0, \infty)}$ follows e.g. from Ref. [20] or [21].

(i) \Rightarrow (ii) Using the algorithm proposed in [23] (see also [29]), one can find that m defined by (II.13) can be uniquely represented as

$$m(z) = \frac{1}{z - a_0 - b_0^2 m_1(z)}, \quad (\text{II.14})$$

where $m_1(z) = \int_{t_3}^{t_4} \frac{d\mu(t)}{t - z}$, is a Nevanlinna function with finite moments. \square

Remark II.2 Already at this point we can say something about the influence of the the measure μ (spectrum of the matrix $H_{[1, \infty)}$) on the position of λ_∞ .

1) Conditions (i) and (ii) in Ref. [21] tell us that $\lambda_\infty \in [t_3, t_4]$ if and only if

$$\int_{t_3}^{t_4} |t - \lambda_\infty|^{-2} d\mu(t) \leq b_0^{-2}, \quad a_0 - \lambda_\infty + b_0^2 \int_{t_3}^{t_4} (t - \lambda_\infty)^{-1} d\mu(t) = 0. \quad (\text{II.15})$$

(In particular, since b_0 is strictly positive, for the first of these conditions to be true, $|t - \lambda_\infty|^{-2}$ needs to be a μ -integrable function; the second condition is just the specialization of eq. (II.9) to the case $z = \lambda_\infty$ and we introduce it here to fully characterize λ_∞ itself). It follows that if the measure μ is sufficiently dense λ_∞ cannot be on $[t_3, t_4]$, i.e. μ “repels” the point λ_∞ . This is the case for Examples III.4 and III.5 below.

2) If instead μ has gaps, these gaps tend to trap λ_∞ . To see this, let’s assume that the spectrum of $H_{[1, \infty)}$ has a gap $(t_5, t_6) \subset [t_3, t_4]$ and that $a_0 \in (t_5, t_6)$. From the definition of $H_{[0, \infty)}$, eq. (I.1), it’s obvious that for $b_0 = 0$ the point a_0 is an eigenvalue of $H_{[0, \infty)}$ with the corresponding eigenvector f satisfying $\langle f | \eta f \rangle \leq 0$, i.e. $a_0 = \lambda_\infty$. We now increase $b_0 = 0$; applying Rouché’s theorem to $-1/m_{[0, \infty)}$ and remembering that if $\lambda_\infty \notin \mathbb{R}$ then $\bar{\lambda}_\infty$ is also an eigenvalue, we see that λ_∞ moves along the real axis until it meets another part of the spectrum of $H_{[0, \infty)}$ (that is either an eigenvalue, or a part of the continuous spectrum, see Ref. [30, 31] for a detailed analysis of a similar problem). This means that if $\lambda_\infty \in (t_5, t_6)$, then for a small change of parameters a_0, b_0 the eigenvalue λ_∞ stays in the gap. We shall see one such case in Example III.6.

As already mentioned, $m_{[0, n]}$ is the $[n/n + 1]$ Padé approximant of $m_{[0, \infty)}$ and it is an \mathcal{N}_1 function for $n \geq 1$. Consequently it can be represented in one of the forms (II.5)–(II.7). As we have just done in Theorem II.1 for $m_{[0, \infty)}$, one can specify this representation:

Proposition II.3 *Each function $m_{[0, n]}$ ($n = 1, 2, \dots$) admits a representation*

$$m_{[0, n]}(z) = \frac{1}{(z - \lambda_n)(z - \bar{\lambda}_n)} \left(z + d_n + \int \frac{d\mu_n(t)}{t - z} \right), \quad (\text{II.16})$$

with $\lambda_n \in \mathbb{C}^+$, $d_n \in \mathbb{R}$ and μ_n a finitely supported measure. Furthermore, the parameters λ_n and d_n and the measure μ_n are uniquely determined and λ_n is the unique eigenvalue of nonpositive type of $H_{[0, n]}$.

The details of the proof of uniqueness can be found e.g. in [26, 27, 32]. The uniqueness in both Theorem II.1 and Proposition II.3 guaranties that λ_n ($n = 1, 2, \dots$) and λ_∞ are properly defined. In the literature they are called the generalized poles of nonpositive type of the corresponding \mathcal{N}_1 function, see [32]. Using the classical result saying that $m_{[1, n]}$ converges to $m_{[1, \infty)}$, see [25, 28, 33], one can prove –via eq. (II.3)– the following convergence result, cf. [20]:

Proposition II.4 *The functions $m_{[0,n]}$ ($n \in \mathbb{Z}_+$) converge to $m_{[0,\infty]}$ as $n \rightarrow \infty$, locally uniformly on $\mathbb{C}_+ \setminus ([t_1, t_2] \cup \{\lambda_\infty\})$.*

Further generalization to different types of η -selfadjoint Jacobi matrices can be found in [20]. As a consequence we have the following corollary (cf. [34]):

Corollary II.5 *The pole λ_n of $m_{[0,n]}$ converges to the pole λ_∞ of $m_{[0,\infty]}$ as $n \rightarrow \infty$.*

Proof. If $\lambda \in \mathbb{C}_+$ or is an isolated eigenvalue then this statement is a simple consequence of Proposition II.4 and the Rouché theorem.

If instead λ_∞ is real and is not an isolated eigenvalue then from Proposition II.4 and the Rouché theorem we see that all the accumulation points of λ_n lie in the spectrum of $H_{[0,\infty]}$, which is a compact set. Since both the functions $m_{[0,n]}$ and $m_{[0,\infty]}$ belong to \mathcal{N}_1 and are of the type (II.6), we have

$$m_{[0,n]}(z) = \frac{1}{(z - \lambda_n)(z - \bar{\lambda}_n)} \varphi_n(z), \quad m_{[0,\infty]}(z) = \frac{1}{(z - \lambda_\infty)(z - \bar{\lambda}_\infty)} \varphi(z),$$

where φ_n and φ are Nevanlinna functions and r_n and r are rational functions. Suppose now that there is a subsequence such that $\lambda_{n_k} \rightarrow \lambda_0 \neq \lambda_\infty$. As a consequence, φ_{n_k} should also converge to a Nevanlinna function $\varphi_0 \neq \varphi$ which contradicts the uniqueness of φ . \square

III. CONVERGENCE RATES

Now we are in a position to ask the principal question of this paper:

What is the character of the convergence of $\lambda_n \rightarrow \lambda_\infty$?

We mainly consider the situation when λ_∞ is simple eigenvalue located outside the support of the measure μ in (II.9): we show a theoretical bound on the convergence rate and test it on examples.

A. Theoretical results

In this section we consider the situation when λ_∞ is a simple pole of m . Note that if $\lambda_\infty \in \mathbb{C}^+$, then it is necessarily a simple pole, due to Theorem II.1 (i); moreover, there exists $n_0 \in \mathbb{N}$ such that $\lambda_n \in \mathbb{C}^+$ for $n > n_0$ (see Theorem A.1 below). If instead λ_∞ is a simple real pole, we show that λ_n is real for sufficiently large n . We begin with a technical result, needed to prove our main theorem.

Proposition III.1 *Let $m = m_{[0,\infty]}$ satisfy the (equivalent) conditions (i), (ii), (iii) of Theorem II.1. If $\lambda_\infty \in \mathbb{C} \setminus [t_3, t_4]$ is a simple pole of m , then*

$$\lambda_\infty - \lambda_n = -\frac{b_0^2 (m_{[1,\infty]}(\lambda_\infty) - m_{[1,n]}(\lambda_\infty))}{1 - b_0^2 m'_{[1,\infty]}(\lambda_\infty)} + \alpha_n,$$

where α_n is such that

$$\frac{\alpha_n}{\sup_{x \in X} |m_{[1,\infty]}(x) - m_{[1,n]}(x)|} \rightarrow 0, \quad n \rightarrow \infty$$

for any disc $X \subseteq \mathbb{C}^+$ containing λ_∞ . If, additionally, $\lambda_\infty \in \mathbb{R}$, then $\lambda_n \in \mathbb{R}$ for sufficiently large n .

Proof. Let X be an open disc, such that $\lambda_\infty \in X \subseteq \mathbb{C}^+ \setminus [t_3, t_4]$. Note that for sufficiently large n the functions

$$m_n(z) := \frac{1}{m_{[0,n]}(z)} = z - a_0 - b_0^2 m_{[1,n]}(z), \quad (\text{III.1})$$

as well as

$$m_\infty(z) = \frac{1}{m_{[0,\infty]}(z)} = z - a_0 - b_0^2 m_{[1,\infty]}(z) \quad (\text{III.2})$$

belong to $\mathcal{C}(X)$, the complex Banach space of continuous functions on X with the supremum norm. Indeed, for sufficiently large n the function $m_{[1,n]}(z)$ has no poles in $X \cap \mathbb{R}$. Also observe that m_n converges to m_∞ in $\mathcal{C}(X)$, since $m_{[1,n]}(z)$ converges to $m_{[1,\infty]}(z)$ locally uniformly on $\mathbb{C} \setminus [t_3, t_4]$. Consider the mapping

$$F : \mathcal{C}(X) \times X \ni (m, x) \mapsto m(x) \in \mathbb{C}.$$

As $\lambda_\infty \in \mathbb{C}^+$ is a simple pole of $m_{[0,\infty]}$, one has

$$m'_\infty(\lambda_\infty) = (-1/m_{[0,\infty]})'(\lambda_\infty) \neq 0.$$

Therefore,

$$\frac{\partial F}{\partial x}(m_\infty, \lambda_\infty) = m'_\infty(\lambda_\infty) \neq 0,$$

and we can apply the implicit function theorem in Banach spaces to the mapping F (see e.g. [35]). As a result we obtain in a neighborhood $U \times Y$ of $(m_\infty, \lambda_\infty)$ a differentiable function $\xi : U \rightarrow Y$ such that

$$\{(m, x) \in U \times Y : m(x) = 0\} = \{(m, \xi(m)) : m \in U\} = 0.$$

We may take Y so small that $Y \subseteq \mathbb{C} \setminus [t_3, t_4]$ and that m_∞ has no other zeros in Y except λ_∞ . Note that for sufficiently large n one has $m_n \in U$. Hence, on one hand we have that for sufficiently large n

$$m_n(\xi(m_n)) = F(m_n, \xi(m_n)) = 0, \quad m_n(x) \neq 0, \quad x \in U \setminus \{\xi(m_n)\}.$$

On the other hand, λ_n converges to λ_∞ and $m_n(\lambda_n) = 0$. Consequently, $\lambda_n = \xi(m_n)$ for n large enough.

Now note that

$$\frac{\partial x}{\partial m}(m_\infty)m = -\frac{\frac{\partial F}{\partial m}(m_\infty, x(m_\infty))m}{\frac{\partial F}{\partial x}(m_\infty, x(m_\infty))} = -\frac{m(\lambda_\infty)}{m'_\infty(\lambda_\infty)}.$$

Furthermore,

$$\begin{aligned} \lambda_\infty - \lambda_n &= \frac{\partial x}{\partial m}(m_\infty)(m_\infty - m_n) + \alpha(m_\infty - m_n) \\ &= -\frac{m_\infty(\lambda_\infty) - m_n(\lambda_\infty)}{m'_\infty(\lambda_\infty)} + \alpha(m_\infty - m_n), \end{aligned}$$

where $\alpha(h_n)/\|h_n\|_{\mathcal{C}(X)} \rightarrow 0$ with $\|h_n\|_{\mathcal{C}(X)} \rightarrow 0$. Set $h_n = m_n - m_\infty$ and

$$\alpha_n = \alpha(m_\infty - m_n) = \lambda_\infty - \lambda_n + \frac{m_\infty(\lambda_\infty) - m_n(\lambda_\infty)}{m'_\infty(\lambda_\infty)}$$

and note that the right-hand side of the above does not depend on the initial choice of the disc X . This finishes the proof of the first statement.

Now let $\lambda_\infty \in \mathbb{R} \setminus [t_3, t_4]$. By the locally uniform convergence of m_n to m_∞ and by the Rouché theorem there is a small disc Z with the center in λ_∞ , such that each function $m_n(z)$ has precisely one zero z_n in Z . As λ_n converges to λ_∞ we must have $\lambda_n = z_n$ for large n . Therefore, $\lambda_n \in \mathbb{R}$, otherwise $\bar{\lambda}_n \in Z$ is another zero of m_n in Z , which is a contradiction. \square

Remark III.2 We are able now to prove the main result of our paper, Theorem III.3. First, though, we would like to stress that there are two equivalent ways of seeing it according to the objects we consider:

A first interpretation takes as its main object the tridiagonal matrix, presented here in a block form

$$H_{[0,\infty]} = \left(\begin{array}{c|ccc} a_0 & -b_0 & 0 & \cdots \\ b_0 & & & \\ 0 & & H_{[1,\infty]} & \\ \vdots & & & \end{array} \right);$$

λ_∞ is then the (unique) eigenvalue of nonpositive type of $H_{[0,\infty]}$, λ_n is the unique eigenvalue of nonpositive type of the finite truncation $H_{[0,n]}$ of $H_{[0,\infty]}$, and the spectrum of $H_{[1,\infty]}$ is contained, by assumption, in $[t_3, t_4]$.

A second interpretation considers instead a meromorphic function $m(z)$ having the representations (II.8) and (II.9) and its $[n - 1/n]$ Padé approximants $m_{[0,n]}$. The point λ_∞ (λ_n) is then the unique pole of nonpositive type of $m(z)$ ($m_{[0,n]}$, respectively).

In both settings Theorem III.3 gives the convergence rate of λ_n to λ_∞ , in terms of the “distance” of λ_∞ from the interval $[t_3, t_4]$: the rate of convergence is at least exponential $\mathcal{O}(q^{-2n})$, where the number q is such that λ_∞ lies on the ellipse with foci at t_3, t_4 and sum of its semi-axes equal to $(t_4 - t_3)q/2$. Consequently, as confirmed by our numerical tests below, the convergence rate gets worse the larger is the eccentricity of said ellipse, i.e.: the convergence slows down when λ_∞ is “close” to the interval $[t_3, t_4]$.

Theorem III.3 *Let $\lambda_\infty, \lambda_n, t_3, t_4$ be as in Theorem II.1 and Remark III.2 above. If $\lambda_\infty \in \mathbb{C} \setminus [t_3, t_4]$ is a simple eigenvalue, then*

$$\limsup_{n \rightarrow \infty} |\lambda_\infty - \lambda_n|^{1/n} \leq \frac{1}{q^2},$$

where $q = g + \sqrt{g^2 - 1}$, and

$$g = \frac{|\lambda_\infty - t_4| + |\lambda_\infty - t_3|}{t_4 - t_3} > 1 \quad (\text{III.3})$$

is the reciprocal of the eccentricity of the ellipse through λ_∞ with foci at t_3, t_4 . If, additionally, $\lambda_\infty \in \mathbb{R}$, then $\lambda_n \in \mathbb{R}$ for sufficiently large n .

Proof. For $R > 1$ let L_R denote the closed set bounded by the ellipse with foci at t_3, t_4 and the sum of its semi-axes equal to $(t_4 - t_3)R/2$. Due to Theorem (2.6.2) in Ref. [36], one has

$$\limsup_{n \rightarrow \infty} \sup_{z \in \mathbb{C} \setminus L_R} |m_{[1,n]}(z) - m_{[1,\infty]}(z)|^{1/n} \leq \frac{1}{R^2}. \quad (\text{III.4})$$

Note that

$$\lambda_\infty \notin L_R \iff R < g + \sqrt{g^2 - 1}. \quad (\text{III.5})$$

Take any $R \in (1, g + \sqrt{g^2 - 1})$ and a small disc X , such that $\lambda_\infty \in X \subseteq \mathbb{C} \setminus L_R$. From Proposition III.1 we obtain that

$$\begin{aligned} |\lambda_\infty - \lambda_n| &\leq C_1 |m_{[1,n]}(\lambda_\infty) - m_{[1,\infty]}(\lambda_\infty)| + \alpha_n \\ &\leq C_2 \sup_{z \in X} |m_{[1,n]}(z) - m_{[1,\infty]}(z)|, \end{aligned}$$

where C_1, C_2 are constants, dependent on $H_{[0,\infty]}$ and X only. As a consequence,

$$\limsup_{n \rightarrow \infty} |\lambda_\infty - \lambda_n|^{1/n} \leq \frac{1}{R^2}.$$

Letting $R \rightarrow g + \sqrt{g^2 - 1}$ finishes the proof. \square

Note that Theorem III.3 cannot be easily generalized to the case when $\lambda_\infty \in [t_3, t_4] \setminus \text{supp } \mu$. For example, if the support of the measure μ consists of two disjoint intervals $[t_3, t_5] \cup [t_6, t_4]$ the estimate (III.4), which was the key point in proving Theorem III.3, still holds only outside the ellipse with foci at t_3, t_4 , the reason being that the union of the poles of the Padé approximants of $\int_{t_3}^{t_4} (t - z)^{-1} \mu(dt)$ may be dense in $[t_5, t_6]$, see for instance Ref. [37].

B. Examples

In our examples we want to be able to choose the position of λ_∞ ; it is therefore convenient to consider cases where it is possible to calculate it without resorting at first to truncated matrices. One way to is look for matrices $H_{[1,\infty]}$ such that the the corresponding functions $m_{[1,\infty]}$ have a closed, analytic form. This will allow us to use (numerical) root finding methods to calculate λ_∞ solving the equation

$$z - a_0 - b_0^2 m_{[1,\infty]}(z) = 0. \quad (\text{III.6})$$

Remembering that

$$m_{[1,\infty)} = \int_{t_3}^{t_4} \frac{d\mu(t)}{t-z}, \quad (\text{III.7})$$

this reduces to finding a suitable measure $\mu(t)$ with finite support.

The choice

$$d\mu = d\sigma_{\alpha,\beta}(t) = \chi_{[-1,1]}(t) \cdot \frac{(1-t)^\alpha(1+t)^\beta dt}{\int_{-1}^1 (1-s)^\alpha(1+s)^\beta ds}, \quad (\text{III.8})$$

where $\chi_{[-1,1]}(t)$ is the characteristic function of the interval $[-1, 1]$, gives us the matrix $H_{[1,\infty)}$ corresponding to Jacobi polynomials with parameters α, β . To construct $H_{[1,\infty)}$ we consider the Jacobi orthogonal polynomials, which form an orthogonal basis in $L^2(\sigma_{\alpha,\beta})$ and the multiplication operator $p \mapsto xp$ in $L^2(\sigma_{\alpha,\beta})$. The three term recurrence relation (4.5.1) and the normalization factors (4.3.3) in Ref. [44] provide the tridiagonal representation $H_{[1,\infty)}$ of the multiplication operator. The spectral theorem for selfadjoint operators guarantees that (III.7) with (III.8) is satisfied.

The choice

$$d\mu = \chi_{[-2,2]}(t) \cdot \frac{\sqrt{4-t^2} dt}{2\pi} \quad (\text{III.9})$$

instead gives the matrix $H_{[1,\infty)}$ with $a_j = 0$, $b_j = 1$, $j = 1, 2, \dots$ corresponding to the orthogonal polynomials associated with the Wigner semicircle measure.

To calculate λ_n we use Matlab [38]: first, we calculate all eigenvalues and eigenvectors of $H_{[0,n]}$; we then find λ_n as the only eigenvalue of nonpositive type of $H_{[0,n]}$, i.e. the only eigenvalue which is either in the upper half-plane or is real with the corresponding eigenvector \mathbf{x} satisfying

$$-|x_0|^2 + \sum_{j=1}^n |x_j|^2 \leq 0.$$

A summary of the relevant results for all our examples can be found in Table I. Only graphs useful to our discussion are shown here; for the remaining cases quoted, pictures can be found in the supplementary files [39]: the file names there refer to those given in Table I.

Example III.4 As our first example we take $\alpha = \beta = 0$ in eq. (III.8) so that

$$m_{[1,\infty)} = \frac{1}{2} \int_{-1}^1 \frac{dt}{t-z} = \frac{1}{2} (\log(1-z) - \log(-1-z)), \quad (\text{III.10})$$

where the branch of the logarithm is chosen in such way that the above function is a Nevanlinna function. In this case $H_{[1,\infty)}$ corresponds, in the way described in the remarks above, to the Legendre polynomials. We now vary the only remaining free parameters a_0 and b_0 of $H_{[0,\infty)}$. Note in any case, due to Remark II.2, we have $\lambda_\infty \notin [t_3, t_4] = [-1, 1]$.

Let us start with $a_0 = 0.5$, $b_0 = 0.05$. It is immediately evident from Figure 1 that the points λ_n arrange themselves on three branches which spiral into λ_∞ . The point λ_n jumps in a regular fashion from one branch to another: all λ_n 's with $n \bmod 3 = \text{const}$ fall on the same branch. The two branches starting on the real axis leave it at $n = 45$ and $n = 190$ respectively, as can be seen from the plot of the imaginary part of λ_n in Figure 2; the plots of the corresponding real parts have each a cusp at the same time, due to the inversion of the direction of motion of λ_n . The plot in Figure 3 shows exponential convergence of λ_n to λ_∞ setting in soon after all three branches leave the real line. The black reference line with slope $-2 \log(q)$ represents the bound from Theorem III.3, the intercept is chosen so that the line is superimposed on the numerical data. In this example (as well as in subsequent examples with measures having no gaps) we see that the estimate of the convergence rate in Theorem III.3 is sharp and consequently can not be improved in general. On the other hand, the estimate is not always sharp, cf. Example III.6.

We have already mentioned that the points λ_n arrange themselves regularly on branches. This behavior is common to most of our examples, except the cases when λ_∞ is on the real axis, where because of Proposition III.1 there is one branch only. Since the branches appear to approach λ_∞ isotropically, as can be e.g. seen in the zoomed picture of Figure 1, this suggests a convenient way of calculating the numerical value of λ_∞ as the mean

$$\lambda_\infty^{(N)} = k^{-1} \sum_{n=N-k+1}^N \lambda_n, \quad (\text{III.11})$$

where k denotes the number of branches and N the last n for which λ_n is calculated.

The value of λ_∞ obtained taking the average of the three last points (one for each branch) equals $0.4999 + 0.0039i$, which agrees well with the value $0.498631 + 0.00391397i$ obtained solving with Mathematica [40] eq. (III.6).

We conclude noting that –here and in all our other examples– the real axis forms a barrier for λ_n : it never crosses it and branches which touch it get stuck in it; this is clearly visible in the movie `Legendre_spirals_a_0.5.avi` that can be found among the supplementary files to this paper [39]. This behavior is related to the symmetry of the spectrum with respect to the real axis.

If we now keep $a_0 = 0.5$ constant and vary b_0 to assume the values $b_0 = 0.5, 0.1$, and 0.01 , in all cases the λ_n 's arrange themselves over three spiraling branches and the value λ_∞ obtained from the average of the last three values of λ_n agrees with the one calculated solving eq. (III.6) with Mathematica to the last digit shown in Table I. In all cases convergence is exponential and the slope of logarithmic plots similar to that in Figure 3 are in agreement with the value $-2\log(q)$ from Theorem III.3 (see Table I). There are some case to case differences, but they do not affect the picture given above: for $b_0 = 0.5$ the three branches are not clearly visible, due to the very fast convergence of λ_n ; for $b_0 = 0.1$ only one branch spends some time on the real axis, up to $n = 46$; and for $b = 0.01$ even after 1000 iterations one of the three branches has not yet left the real axis (for figures see the supplementary material [41]).

Our last example with measure eq. (III.10) is a case when $\lambda_\infty \in \mathbb{R} \setminus [t_3, t_4]$: if we take $a_0 = 1.001$ and $b_0 = 0.001$ we get $\lambda_\infty \simeq 1.001$ (Mathematica has problems solving eq. (III.6) in this case). The values of λ_n are all real; we therefore have a single branch. Convergence is again exponential (for figures see the supplementary material [42]). It is instructive to compare this case to the case $a_0 = 0.5$, $b = 0.05$: the distance of λ_∞ from the interval $[-1, 1]$ is of the same order, but the convergence is much faster in the present case. This is due to the different eccentricities of the ellipses from Theorem III.3: in the present case the eccentricity is smaller, and therefore q is larger and in consequence the convergence rate is better.

Finally, in Figure 4 we summarize the convergence behavior when submatrix $H_{[1,\infty)}$ corresponds to measure eq. (III.10): we vary the parameters $a_0 \in (-1, 1)$ and $b_0 \in (0.05, 0.5)$ and for each pair (a_0, b_0) we compute the value n_0 where the last λ_n branch leaves the real axis. Each pair (a_0, b_0) determines a single point λ_∞ in the upper half-plane, which we plot color coded according to n_0 . The figure appears to have a fractal character for which we do not yet have an explanation but which we suspect to be related to the way the number of λ_n branches varies with varying a_0 . This can be seen in the movie `Legendre_spirals_b_0.01.avi` [39] where we keep $b_0 = 0.01$ and vary a_0 . We instead observe no change in the number of branches when varying b_0 at constant a_0 (see e.g. the movie `Legendre_spirals_a_0.5.avi` [39]).

As we have already mentioned, branches are a common occurrence, not limited to the example just given. We give here a couple more examples.

Example III.5 We now take $H_{[1,\infty)}$ corresponding to the orthogonal polynomials associated with the Wigner semi-circle measure, i.e. the measure given by eq. (III.9) and we choose $a_0 = 0.5$, $b_0 = 0.1$ as the remaining parameters for $H_{[0,\infty)}$. Note due to Remark II.2 we again have $\lambda_\infty \notin [t_3, t_4] = [-2, 2]$.

In Figure 5 it is possible to see that the λ_n 's form twelve branches. Knowing this, we can use the recipe given above to calculate λ_∞ as the mean eq. (III.11) of the last twelve values of λ_n ; the result agrees to the last digit shown in Table I with the value obtained solving eq. (III.6) with Mathematica.

Figure 6 shows exponential convergence of λ_n to λ_∞ with the rate predicted by Theorem III.3; other plots concerning this example can be found as supplementary files [43].

The video `Wigner_spirals_b_0.01.avi` in [39] shows the evolution of the λ_n branches under the change of the parameter a_0 . As in Example III.4, it is evident that here too the number of branches changes with a_0 . Looking at the first few frames of the movie it is also evident that there are branches that start off the real axis, hit it and –instead of continuing into \mathbb{C}^- – get trapped in it moving horizontally for a number of n , and then leave it when the spiral reenters \mathbb{C}^+ .

Example III.6 Here we present an example of a different nature. The matrix $H_{[1,\infty)}$ is constructed in such way, that its spectrum is a totally disconnected, Cantor-like set, see [45] for details; the other parameters are $a_0 = 0.5$ and $b_0 = 0.1$. In this particular case we could count 27 branches of λ_n ; such a high number is hardly visible when plotting λ_n in the complex plane but can be seen in the plot of $\log|\lambda_n - \lambda_\infty|$ in Figure 7: the λ_n 's form regular clusters of 27 points.

What is particularly noteworthy is that –contrary to the previous examples– the convergence rate is faster than the one predicted by Theorem III.3, as can be seen comparing the theoretical bound (black line) with the numerical points in Figure 7. This is probably due to the fact that the spectrum of $H_{[1,\infty)}$ contains gaps. Other pictures corresponding to this example (called `Cantor_a_0.5_b_0.1_xxx.eps`), as well as the video `Cantor_spirals_b_0.2.avi` showing the evolution of branches under the change of the parameter a_0 , can be found in the supplementary files [39]: again the number of branches changes with a_0 ; moreover intervals in a_0 where both λ_∞ and all the λ_n become real are evident and correspond to the gaps in $H_{[1,\infty)}$, see Remark II.2.

Although Theorem III.3 proves the exponential rate of convergence of λ_n to λ_∞ , it does not say when this convergence starts manifesting itself: at least in theory we could have $|\lambda_\infty - \lambda_n| > q^{-2n}$ for some n . Our numerical tests indicate that the convergence is somehow “better” than the above bound, as the asymptotic behavior is $K \cdot q^{-2n}$ with $K < 1$. Even the curious initial behavior connected with the real axis we observed in several cases above, does not bring $|\lambda_\infty - \lambda_n|$ to exceed q^{-2n} . On the other hand it would be convenient to have an estimate of n_0 such that for $n > n_0$ the point λ_n is sure to be outside the support $[t_3, t_4]$ of the measure μ : if one or more of the λ_n ’s branches is still on $[t_3, t_4]$, our justification for estimating λ_∞ by the mean eq. (III.11) is compromised. We give an upper bound for n_0 in Appendix A.

C. $\lambda_\infty \in \mathbb{R}$ is embedded in the spectrum of the representing measure

We shall limit our investigation of the case when $\lambda_\infty \in [t_3, t_4]$ to an example where $\lambda_\infty = t_3$, to show that convergence in this case is in general worse than exponential. To build our example, we start by recalling Remark II.2. The only example known to us of classical orthogonal polynomials satisfying condition (II.15) with $\lambda_\infty \in [t_3, t_4]$ are the Jacobi polynomials with parameters $\alpha \geq 2$ or $\beta \geq 2$ and with $\lambda_\infty = t_3$ or $\lambda_\infty = t_4$, respectively.

Example III.7 We take $H_{[1, \infty)}$ such that

$$m_{[1, \infty)} = \int_{-1}^1 \frac{\frac{3}{4}(1+t)^2(1-t)dt}{t-z},$$

i.e. we take $\alpha = 2, \beta = 1$ in eq. (III.8). We then choose $a_0 = -5/3, b_0 = \sqrt{2/3}$, so that $\lambda_\infty = -1$. This can be seen e.g. by analyzing the matrix $H_{[0, \infty)}$ itself: it results from [21] conditions (i) and (ii) that -1 is an algebraically simple eigenvalue of $H_{[0, \infty)}$ with the corresponding eigenvector x satisfying $-|x_0|^2 + \sum_{j=1}^{\infty} |x_j|^2 = 0$, i.e. $\lambda_\infty = -1$ is the unique eigenvalue of nonpositive type of $H_{[0, \infty)}$.

Furthermore, due to Theorem 2.2 (p_{1s}) of [21], -1 is a singular critical, algebraically simple eigenvalue (see [21] for a classification of eigenvalues of nonpositive type).

The log-log plot of $|\lambda_n - \lambda|$ Vs. n in Figure 8 shows clearly that convergence in this case is only polynomial: $|\lambda_n - \lambda| \simeq n^{-2}$, as can be seen comparing the numerical data with the black reference line whose slope is -2 . The plot of the real and imaginary part of λ_n can be found in [39] as the file `Jacobi12crit_ReIm.eps`.

IV. CONCLUDING REMARKS

As already stated above, the main question we tried to answer here is: “Suppose we are only able to compute the spectrum of finite truncations of a pseudo-Hermitian tridiagonal matrix $H_{[0, \infty)}$; can we say something about the spectrum of the full operator $H_{[0, \infty)}$? Most interestingly, can we predict if the spectrum of $H_{[0, \infty)}$ is real or not?”

Suppose we have performed N iterations, increasing step by step the size of the truncated matrix $H_{[0, n]}$; one of the next four cases applies.

- λ_n is real for all $n = 1, \dots, N$, is either the minimum or the maximum of the spectrum of $H_{[0, n]}$ and is separated from the other eigenvalues. Then the limit point λ_∞ is also a real single eigenvalue, separated from other eigenvalues of $H_{[0, \infty)}$.
- λ_n is complex for all n larger than a $n_0 < N$. Then the limit point λ_∞ is also a complex single eigenvalue. λ_∞ itself can be evaluated by finding the number of λ_n branches and then using eq. (III.11).
- λ_n oscillates between the real line and the complex plane up to $n = N$, a common occurrence when λ_∞ is very close to the support of the measure μ . Then the situation is in principle unclear: the limit eigenvalue λ_∞ might be a complex point, a real critical point, or a real point in a relatively small gap of the spectrum. Still, if the λ_n branches can be found and not too many of them are still trapped on \mathbb{R} for $n \simeq N$, it is still possible to give a numerical evaluation $\lambda_\infty^{(N)}$ of λ_∞ by a careful use of eq. (III.11). If the plot of $\log |\lambda_n - \lambda_\infty^{(N)}|$ is then approximately a straight line, this is another indication for λ_∞ being a simple eigenvalue out of the support of μ .
- The sequence λ_n converges to a point $\lambda_\infty \in \mathbb{R}$, but the convergence is not exponential, which again can be seen by the study of the plot of $\log |\lambda_n - \lambda_\infty|$. Then λ_∞ is a critical point on the real line, embedded in the

support of μ . In view of the second equation of (II.15), this case seems to be non-generic, i.e. a small change of the entries of the matrix will lead to a different case. However, we were able to clearly observe this case in a numerical simulation, which in our opinion is an argument for considering this possibility as well.

While, for sake of simplicity, we restricted ourselves to the case of matrices with a single eigenvalue of nonpositive type, we believe that the results derived above can be generalized to a wider class of operators, at least to those considered in Ref. [20].

In the context of random matrices [47] or Nevanlinna functions, our research can be viewed as concerning the problem of predicting whether or not $\lambda_\infty \in [t_3, t_4]$ by calculating a finite number of Padé approximants. A connection can also be found to Padé approximation of the Z-transform, considered in [48], where the real line is replaced by the unit circle.

Acknowledgments

Michał Wojtylak gratefully acknowledges the financial assistance of the Alexander von Humboldt Foundation with a Research Grant for Experienced Scientists, carried out at TU Berlin and with a Return Home Scholarship, carried out at Jagiellonian University, Kraków. Maxim Derevyagin gratefully acknowledges the financial assistance of the European Research Council under the European Union Seventh Framework Programme (FP7/2007-2013)/ERC, grant agreement no. 259173. Maxim Derevyagin and Michał Wojtylak are indebted to Professor Olga Holtz for her encouragement and support.

Appendix A: Estimate of the maximum number of real λ_n , when $\lambda_\infty \in \mathbb{C}^+$

Theorem A.1 *Let $m = m_{[0, \infty)}$ be of the forms (II.8) and (II.9) with $\lambda_\infty \in \mathbb{C}^+$. Then for any $\varepsilon \in (0, 1)$ for*

$$n > N_\varepsilon := \frac{\log \left(\frac{8b_0^2 g \max_{z \in gL_R} |m_{[0, \infty)}(z)|}{(g-1)^2(t_4-t_3)} \right)}{\log \left(1 + \varepsilon \sqrt{1-g^{-2}} \right)} \quad (\text{A.1})$$

one has

$$\lambda_n \in \mathbb{C} \setminus L_{R(\varepsilon)},$$

where g is again given by eq. (III.3), $R(\varepsilon) = g + \varepsilon \sqrt{g^2 - 1}$ and $L_{R(\varepsilon)}$ again denotes the closed set bounded by the ellipse with foci at t_3, t_4 and the sum of its semi-axes equal to $(t_4 - t_3)R(\varepsilon)/2$. In particular, if $n > N_\varepsilon$ for some $\varepsilon \in (0, 1)$ then $\lambda_n \notin [t_3, t_4]$.

Proof. Consider the functions

$$m_n(z) := \frac{1}{m_{[0, n]}(z)}, \quad m_\infty(z) = \frac{1}{m_{[0, \infty)}(z)}.$$

We now recall the estimate given in [36] as formula (6.10): for every $n \in \mathbb{Z}_+$ and for every $\delta \in (1, R)$ one has

$$\max_{z \in \partial L_R} |m_{[1, \infty)}(z) - m_{[1, n]}(z)(z)| \leq \frac{8\delta}{(t_4 - t_3)(\delta - 1)^2} \left(\frac{\delta}{R} \right)^{2n}. \quad (\text{A.2})$$

Applying equation (A.2) with $\delta = g$, $R = R(\varepsilon) = g + \varepsilon \sqrt{g^2 - 1}$ we get after elementary transformations of (A.1) that

$$\begin{aligned} |m_n(z) - m_\infty(z)| &= b_0^2 |m_{[1, n]}(z) - m_{[1, \infty)}(z)| \\ &\leq \frac{8b_0^2 g}{(t_4 - t_3)(g - 1)^2} \left(\frac{g}{1 + \varepsilon \sqrt{g^2 - 1}} \right)^{2n} \\ &\leq \frac{1}{\max_{z \in \delta L_R} |m_{[0, \infty)}(z)|} = \min_{z \in \delta L_R} |m_\infty(z)|. \end{aligned}$$

Hence, by the the Rouche theorem, m_n and m_∞ have the same number of zeros in $\bar{\mathbb{C}} \setminus L_R$. However, m_∞ has precisely two zeros in $\bar{\mathbb{C}} \setminus L_R$, namely λ_∞ and $\bar{\lambda}_\infty$. As λ_n is the only a zero of m_n in the upper half-plane, we get $\lambda_n \in \mathbb{C} \setminus L_R$. \square

If we now apply Theorem A.1 to Example III.4, we get $N_{0.5} = 52$ for $b_0 = 0.5$, $N_{0.5} = 2155$ for $b_0 = 0.1$, $N_{0.5} = 10917$ for $b_0 = 0.05$, and $N_{0.5} \simeq 4 \cdot 10^5$ for $b_0 = 0.01$. Comparing with Example III.4, where $n_0 \simeq 1, 46, 190$, and $n_0 \gg 1000$ respectively, we see that the estimate $N_{0.5}$ is a far from tight upper bound whose ratio to the numeric value n_0 appears to grow with decreasing b_0 .

-
- [1] There are in practice some rare exceptions when a real spectrum is not sought – as for example when looking for resonances through complex dilatation of a Hamiltonian [49] – and it has to be kept in mind that, even when the Hamiltonian can be made to be Hermitian by symmetrization, different linear combinations of orderings of the operators in the Hamiltonian itself can be possible (see e.g. the case of the double pendulum [50]) corresponding to different physical systems having the same classical Hamiltonian.
- [2] see any quantum mechanics text, e.g. P. Dirac, “The Principles of Quantum Mechanics” Oxford University Press, Oxford, 4th ed. (1958).
- [3] C.M. Bender and S. Boettcher, Phys. Rev. Lett. 80 (1998) 5243.
- [4] Under T reflection one replaces i by $-i$ in the operator while under P reflection one replaces x by ax , where $a/2$ is the origin about which one is performing the parity reflection.
- [5] A. Bohr and B.R. Mottelson, Nuclear Structure, Vol. I, Sect. 2.4, (W.A. Benjamin Inc., New York, 1969).
- [6] C. Itzykson and J.-M. Drouffe, Statistical field theory, Vol. 1, Sect. 3.2.3, (Cambridge University Press, Cambridge, 1989).
- [7] H. Feshbach, C. E. Porter and V. F. Weisskopf, Phys. Rev. 96 448 (1954).
- [8] J. Feinberg and A. Zee, cond-mat/9706218.
- [9] M.V. Berry and D.H.J. O’Dell, J. Phys. A 31 (1998) 2093.
- [10] C. M. Bender, G. V. Dunne, and P. N. Meisinger, “Complex periodic potentials with real band spectra” Phys. Lett. A 252 (1999) 272.
- [11] R. Nevanlinna, Ann. Ac. Sci. Fenn. 1 (1952) 108; 163 (1954) 222; L.K. Pandit, Nuovo Cimento (supplemento) 11 (1959) 157; E.C.G. Sudarshan, Phys. Rev. 123 (1961) 2183; M.C. Pease III, Methods of matrix algebra (Academic Press, New York, 1965); T.D. Lee and G.C. Wick, Nucl. Phys. B 9 (1969) 209; F.G. Scholtz, H. B. Geyer and F.J.H. Hahne, Ann. Phys. 213 (1992) 74.
- [12] J. Bognár, *Indefinite Inner Product Spaces*, Springer-Verlag, New York-Heidelberg, 1974.
- [13] I.S. Iohvidov, M.G. Krein, H. Langer, *Introduction to spectral theory of operators in spaces with indefinite metric*, Mathematical Research, vol. 9. Akademie-Verlag, Berlin, 1982.
- [14] I. Gohberg, P. Lancaster and L. Rodman: *Indefinite Linear Algebra and Applications*. Birkhäuser-Verlag, 2005.
- [15] A. Mostafazadeh, J. Math. Phys. 43 (2002) 205; 43 (2002) 2814; 43 (2002) 3944.
- [16] Z. Ahmed, Phys. Lett. A 290 (2001) 19.
- [17] Z. Ahmed, Phys. Lett. A 294 (2002) 287.
- [18] Stefan Weigert; “An algorithmic test for diagonalizability of finite-dimensional PT-invariant systems” J. Phys. A: Math. Gen. 39 (2006) 235245.
- [19] L.S. Pontryagin, Hermitian operators in spaces with indefinite metric, *Izv. Nauk. Akad. SSSR, Ser. Math.* 8 (1944), 243–280 [Russian].
- [20] M.S. Derevyagin, V.A. Derkach, “On the convergence of Padé approximations for generalized Nevanlinna functions”, *Trans. Moscow Math. Soc.* 68 (2007) 2007, 119–162.
- [21] P. Jonas and H. Langer, “A model for π -selfadjoint operator in a Π_1 space and a special linear pencil”, *Integr. Equ. Oper. Th.* 8 (1985), 13–35.
- [22] P. Jonas, H. Langer, B. Textorius, “Models and unitary equivalence of cyclic selfadjoint operators in Pontrjagin spaces”, *Operator Theory: Advances and Applications*, 59 (1992), 252–284.
- [23] M.S. Derevyagin, “On the Schur algorithm for indefinite moment problem”, *Methods of Functional Analysis and Topology*, Vol. 9 (2003), No.2, 133–145.
- [24] M. Derevyagin, V.Derkach, “Spectral problems for generalized Jacobi matrices”, *Linear Algebra Appl.*, Vol. 382 (2004), 1–24.
- [25] F. Gesztesy, B. Simon, “ m -functions and inverse spectral analysis for finite and semi-infinite Jacobi matrices”, *Journal d’Analyse Math.* 73 (1997) 267–297.
- [26] V. Derkach, S. Hassi, and H.S.V. de Snoo, “Operator models associated with Kac subclasses of generalized Nevanlinna functions”, *Methods of Functional Analysis and Topology*, 5 (1999), 65–87.
- [27] A. Dijksma, H. Langer, A. Luger, and Yu. Shondin, “A factorization result for generalized Nevanlinna functions of the class \mathbf{N}_κ ”, *Integral Equations Operator Theory*, 36 (2000), 121–125.
- [28] N.I. Achiezer, *The classical moment problem*, Oliver and Boyd, Edinburgh, 1965.
- [29] D. Alpay, A. Dijksma, H. Langer, “The Transformation of Issai Schur and Related Topics in an Indefinite Setting, System Theory, the Schur Algorithm and Multidimensional Analysis Operator Theory: Advances and Applications Volume 176,

- 2007, 1–98.
- [30] H.S.V. de Snoo, H. Winkler, M. Wojtylak, Zeros of nonpositive type of generalized Nevanlinna functions with one negative square, *J. Math. Anal. Appl.*, 382 (2011), 399–417.
- [31] H.S.V. de Snoo, H. Winkler, M. Wojtylak, Global and local behavior of zeros of nonpositive type, *J. Math. Anal. Appl.*, 414 (2014) 273–284 .
- [32] H. Langer, “A characterization of generalized zeros of negative type of functions of the class \mathbf{N}_κ ”, *Oper. Theory Adv. Appl.*, 17 (1986), 201–212.
- [33] B. Simon, “The classical moment problem as a self-adjoint finite difference operator”, *Adv. Math.*, 137 (1998), 82–203.
- [34] H. Langer, A. Luger, V. Matsaev, “Convergence of generalized Nevanlinna functions”, *Acta Sci. Math. (Szeged)*, 77 (2011), 425–437.
- [35] S.G. Krantz, H.R. Parks, *The Implicit Function Theorem: History, Theory, and Applications*, Springer Science+Business Media, 2013.
- [36] E.M. Nikishin, V.N. Sorokin, *Rational approximations and orthogonality*, Translations of Mathematical Monographs, 92. American Mathematical Society, Providence, RI, 1991.
- [37] S. P. Suetin, “On the dynamics of ”wandering” zeros of polynomials that are orthogonal on certain intervals”, *Russian Mathematical Surveys* 57(2), 425–427.
- [38] MATLAB, R2014b, The MathWorks, Inc., USA.
- [39] <http://www2.im.uj.edu.pl/MichalWojtylak/convergence.html>
- [40] Mathematica, 10.0, Wolfram Research, Inc., USA.
- [41] The pictures names in [39] are `Legendre_a_0.5_b_0.xxx_compl.eps` for λ_n on the complex plane, `Legendre_a_0.5_b_0.xxx_ReIm.eps` for real and imaginary part of λ_n , and `Legendre_a_0.5_b_0.xxx_conv.eps` for the logarithmic plot for the convergence rate.
- [42] The pictures names in [39] are `Legendre_a_1.001_b_0.001_xxxx.eps` for λ_n on the complex plane (`xxxx=compl`), real and imaginary part of λ_n (`xxxx=ReIm`), and the convergence rate (`xxxx=conv`).
- [43] The names are `Wigner_a_0.5_b_0.1_xxxx.eps`.
- [44] G. Szego, *Orthogonal polynomials*, AMS, Providence, Rhode Island, 1939.
- [45] M.F. Barnsley, J.S. Geronimo, N.A. Harrington, “Infinite-dimensional Jacobi matrices associated with Julia sets”, *Proc. AMS*, 88 (1983), 625–630.
- [46] J. Wimp, “Explicit formulas for the associated Jacobi polynomials and some applications”, *Can. J. Math.*, 39(1987), 983–1000.
- [47] M. Wojtylak, “On a class of H -selfadjoint random matrices with one eigenvalue of nonpositive type” *Electron. Commun. Probab.* 17 (2012), no. 45, 114.
- [48] D. Bessis, R. Perotti, Universal analytic properties of noise: introducing the J-matrix formalism, *J. Phys. A: Math. Theor.* 42 (2009) 365–202.
- [49] A. Buchleitner and D. Delande, *Phys. Rev. Lett.* **70**, 33 (1993).
- [50] L. C. Perotti, *Phys. Rev.* **E70**, 066218 (2004).

| | a_0 | b_0 | $\max n$ | λ_∞ | n_0 | q | $ \lambda_\infty - \lambda_n $ |
|-------------|-------|--------------|----------|--------------------|----------|--------|--------------------------------|
| Legendre | 0.5 | 0.5 | 50 | $0.4045 + 0.3064i$ | 1 | 1.3855 | $\simeq q^{-2n}$ |
| | 0.5 | 0.1 | 200 | $0.4946 + 0.0155i$ | 46 | 1.0180 | $\simeq 3.5^{-1} q^{-2n}$ |
| | 0.5 | 0.05 | 1000 | $0.4986 + 0.0039i$ | 190 | 1.0045 | $\simeq 4.6^{-1} q^{-2n}$ |
| | 0.5 | 0.01 | 1000 | $0.4999 + 0.0002i$ | > 1000 | 1.0002 | $\simeq 6.5^{-1} q^{-2n}$ |
| | 1.001 | 0.001 | 200 | 1.0010 | — | 1.0456 | $\simeq 12.5^{-1} q^{-2n}$ |
| Wigner | 0.5 | 0.1 | 1000 | $0.4975 + 0.0096i$ | 175 | 1.0050 | $\simeq 4^{-1} q^{-2n}$ |
| Cantor | 0.5 | 0.1 | 400 | $0.5074 + 0.0096i$ | 81 | 1.0044 | $\ll q^{-2n}$ |
| Jacobi(1,2) | -5/3 | $\sqrt{2/3}$ | 300 | -1 | — | 1 | $\simeq n^{-2}$ |

TABLE I: Parameters and numerical results for Examples III.4, III.5, III.6 and III.7. If $\lambda_\infty \notin \mathbb{R}$ then n_0 denotes the maximal n for which $\lambda_n \in \mathbb{R}$, q was computed according to Theorem III.3.

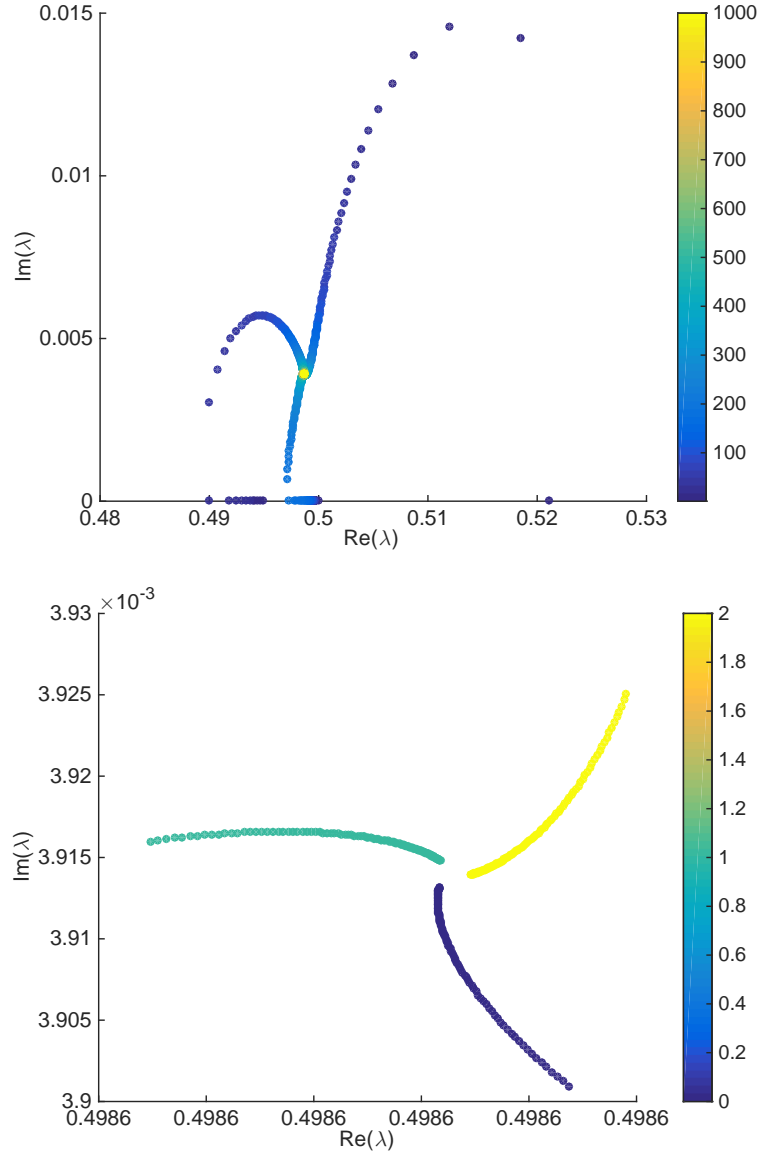


FIG. 1: The only eigenvalue λ_n of nonpositive type of the matrix $H_{[0,n]}$ given in eq. (I.2) with $a_0 = 0.5$, $b_0 = 0.05$ and $H_{[1,n]}$ being the Jacobi matrix corresponding to the Legendre polynomials. The points, each corresponding to a different n , are plotted on the complex plane color coded according to n in the upper picture, and according to $n \bmod 3$ (0–blue, 1–cyan, 2–yellow) in the lower picture, where we show a zoomed detail around λ_∞ . The three branches of λ_n mentioned in the text are clearly visible. See Example III.4.

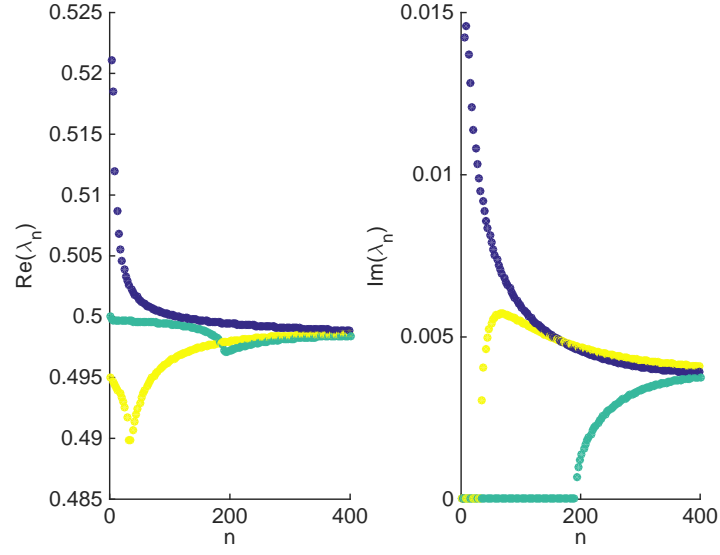


FIG. 2: Real and imaginary part of the eigenvalue λ_n from Figure 1 Vs. n . The points color coded according to $n \bmod 3$. The cusps in the real parts of the yellow and cyan branches correspond to the change of direction when a branch leaves the real line, see Figure 1. See Example III.4.

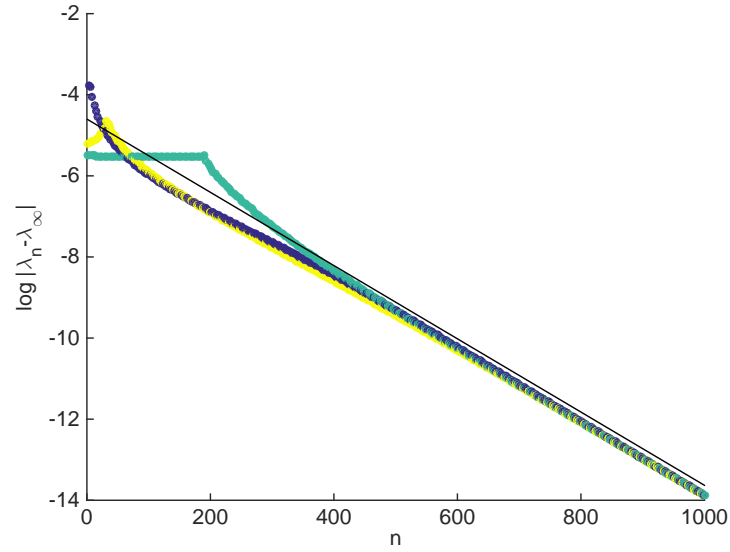


FIG. 3: Same parameters as in Figure 1. The black line represents the theoretical bound given in Theorem III.3, shifted down so as to be superimposed on the numerical data. The logarithmic scale on the vertical axis makes evident the exponential convergence of λ_n to λ_∞ . See Example III.4.

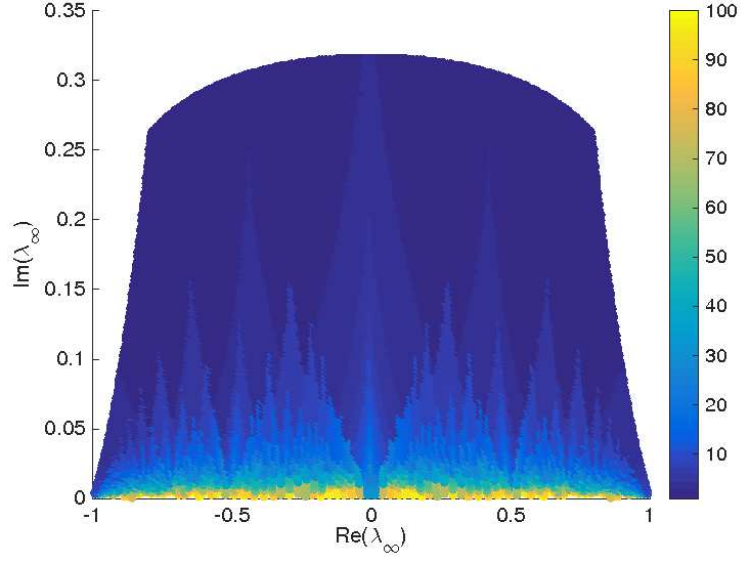


FIG. 4: The value n_0 where the last λ_n branch leaves the real axis as a function of λ_∞ . $H_{[1,n]}$ is the Jacobi matrix corresponding to the Legendre polynomials and a_0 and b_0 vary to get the different values of λ_∞ . See Example III.4.

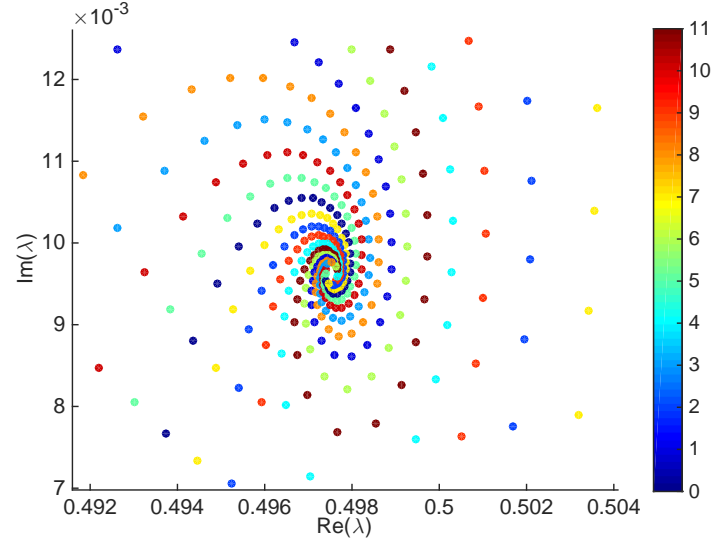


FIG. 5: The eigenvalues λ_n for $H_{[1,n]}$ associated with the Wigner measure and parameters $a_0 = 0.5$, $b_0 = 0.1$, plotted in the complex plane, color coded according to $n \bmod 12$ where twelve is the number of λ_n branches. See Example III.5.

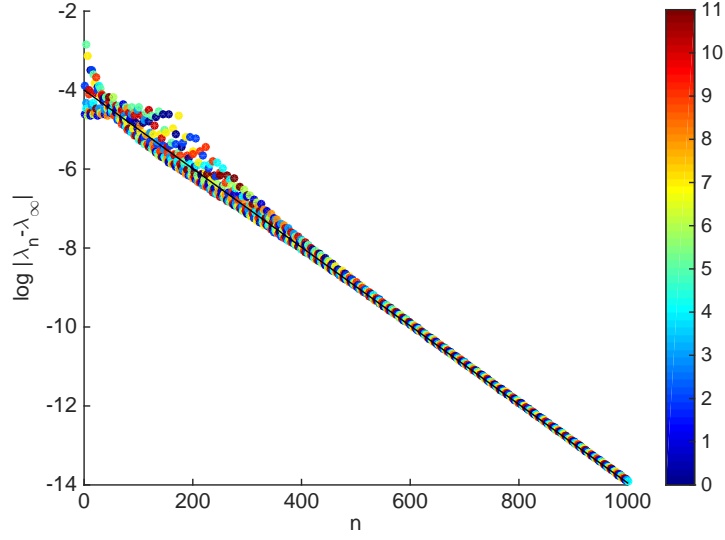


FIG. 6: Same parameters and color code as in Figure 5. The black line represents the theoretical bound given in Theorem III.3, shifted down so as to be superimposed on the numerical data. The logarithmic scale on the vertical axis makes evident the exponential convergence of λ_n to λ_∞ . See Example III.5.

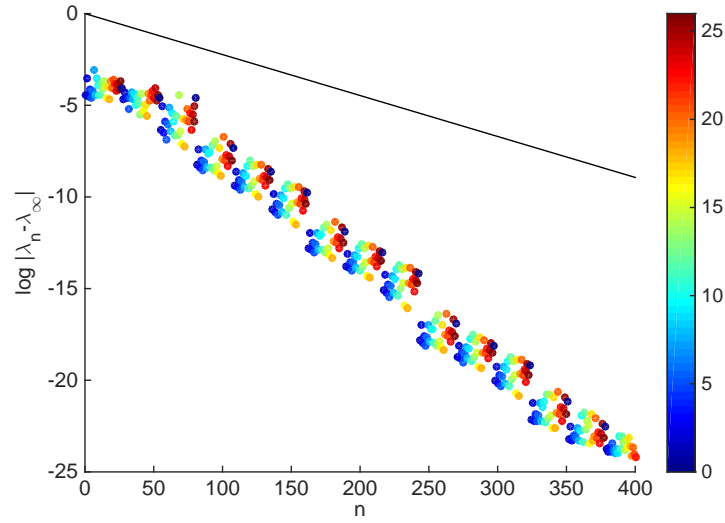


FIG. 7: Exponential convergence of λ_n to λ_∞ . Here $H_{[1,\infty)}$ is associated with a measure on a Cantor-like set and $a_0 = 0.5$, $b_0 = 0.1$. The black line represents the theoretical bound given in Theorem III.3. Color coding according to $n \bmod 27$ evidences a repeated pattern of 27 points. The observed convergence is again exponential but much faster than the bound given by Theorem III.3: the observed q is approximately 1.1147, much larger than the theoretical one 1.0044. See Example III.6.

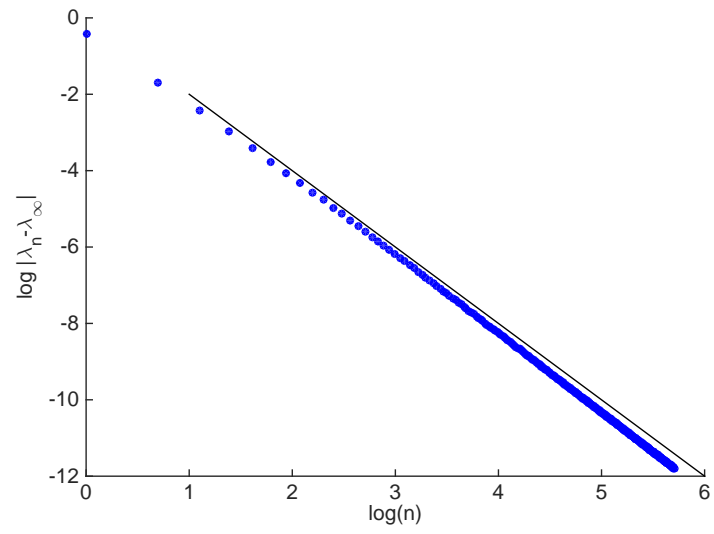


FIG. 8: Log-log plot showing $\mathcal{O}(n^{-2})$ convergence of λ_n to $\lambda_\infty = -1$ in a case when λ_∞ is embedded in the spectrum of $H_{[1,\infty)}$. See Example III.7.